Research Article

Journal of Environmental Nanotechnology

Contrastive Analysis of Interferometric Techniques for Small Channel Temperature Measurements

H. Divya[1*] and L. B. Gantala[2]

[1]Department of Physics, Saveetha School of Engineering, Saveetha Institute of Medical and Technical Sciences (SIMATS), Chennai, TN, India
[2]Department of Research and Innovation, Saveetha School of Engineering, Saveetha Institute of Medical and Technical Sciences (SIMATS), Chennai, TN, India
Received: 31.01.2024 Accepted: 12.03.2024 Published: 30.03.2024
*divyaharidask@gmail.com

ABSTRACT

This research employs a state-of-the-art digital interferometric technique to investigate the temperature distribution within a confined rectangular channel, with a hydraulic diameter of 3 mm. The experimental setup incorporates an optical glass channel, with nanofluids (Aluminium oxide) as the test fluid at 0.001% volume concentration. To induce controlled heating, a heater filament is strategically placed along the bottom wall of the channel. Simultaneously, a T-type thermocouple is carefully placed to measure the temperature along the upper wall. Two distinct interferometric methods, namely the Michelson interferometer and the Mach-Zehnder interferometer, are employed to capture the complex details of fringes resulting from the evolving temperature field within the test section. A high-resolution CCD camera is employed to capture these fringes, and sophisticated digital image processing techniques are subsequently applied for in-depth fringe analysis. The culmination of these efforts results in the origin of a comprehensive localized temperature distribution map within the small-sized channel. The obtained temperature profiles are meticulously compared, providing valuable insights into the effectiveness and reliability of the Michelson and Mach-Zehnder interferometric techniques in this specific experimental context. This detailed comparative analysis contributes to the broader understanding of interferometric methods for temperature measurements in confined fluidic systems.

Keywords: Interferometry; Compact channels; Nanofluids; Heat transfer.

NOMENCLATURE

LIST OF SYMBOLS	
C	Gladstone Dale constant, m^3/kg
Dh	Hydraulic diameter, m
h	Heat transfer coefficient, $Wm^{-2}K^{-1}$
k	Thermal conductivity, $Wm^{-1}K^{-1}$
L	Width of channel, m
n	Refractive index
Nu	Nusselt number
q	Heat flux at the bottom of the heat sink, Wm^{-2}
S	Fringe number
T	Temperature, K

GREEK SYMBOLS	
ρ	Density, kgm^{-3}
λ	Wavelength, m

SUBSCRIPTS AND SUPERSCRIPTS	
av	Average
f	Film
m	Mean value
r	Reference
w	Wall
x	Location along x coordinate

1. INTRODUCTION

The rapid miniaturization of electronic devices has increased the demand for developing methods to dissipate heat from them. The recent advancements in the compact and effective industry can increase the system heat dissipation up to 1000 W/cm^2 in the immediate future (Lee and Mudawar, 2009). It is proven that almost 50% of the device malfunction is caused by the ineffective heat dissipation from the electronic systems and components (Pedram *et al*. 2006). Fluid flow through small-sized channels has been proposed as a solution for the dissipation of heat fluxes from smaller and faster electronic components (Pease and Tuckerman, 1981; Wei and Joshi, 2004; Mohammed *et al.* 2011). The influence of channel shape on the thermal and hydraulic performance of microchannel heat sink was investigated by Mohammed *et al.* 2011. Accurate measurement of temperature and heat transfer parameters in such channels is required to design efficient heat dissipation channels. Even though extensive research is reported on these channels, the results obtained are non-conclusive, demanding further investigations in this area. This discrepancy in local variations in temperature gradients and related heat transfer are majorly due to the intrusive nature of the measurement technique itself. In small scale channels, the measurement systems often replace the

system to a new system due to its presence and the resulting flow disturbances, conduction effects, formation of secondary vortexes, etc.

Optical methods have proven to be exceptionally versatile in the realm of quantitative measurements of thermal phenomena. This versatility arises from their unique ability to facilitate real-time, non-intrusive analysis across the entire optical field, enabling researchers to gain valuable insights into the intricacies of heat distribution and temperature changes in various materials and environments (Dennis *et al*. 2006; Merzkirch and Wolfgang, 2006; Cardone and Gennaro, 2010; Ayoub *et al*. 2019). The key advantage of optical methods lies in their non-intrusiveness, meaning that they do not interfere with the studied system. Traditional methods, such as contact-based sensors or thermocouples, can sometimes perturb the system being analyzed, leading to inaccuracies or disturbances in the thermal field. In contrast, optical methods allow for observation without direct physical contact, ensuring that the measurements are as minimally disruptive as possible. This characteristic is especially important when studying delicate or complex thermal processes where even minor disturbances can influence the results. Real-time analysis is another crucial aspect of optical methods in thermal measurements. The ability to capture and process data in real-time provides a dynamic understanding of how thermal phenomena evolve over time. This is particularly beneficial in applications where rapid changes in temperature occur, such as in industrial processes, electronic devices, or dynamic thermal systems. Optical methods, therefore, offer a valuable tool for monitoring and controlling thermal processes in situations where timing is critical. The continuous advancements in technology have significantly contributed to the efficacy of optical methods for thermal analysis (Jagadesh *et al*. 2023; Gannavarpu *et al*. 2018; Mirko *et al.* 2020). The development of fast and sophisticated image-capturing devices has improved the resolution, speed and sensitivity of optical measurements. High-speed cameras, for example, enable researchers to capture rapid temperature changes and dynamic thermal events with precision. This technological progress is instrumental in expanding the range of applications for optical methods, allowing researchers to delve into previously inaccessible realms of thermal analysis.

The utilization of optical methods in the investigation of thermal phenomena is particularly significant, and among these methods, the 'index of refraction method' stands out prominently. This method involves leveraging interferometric techniques, with specific emphasis on the detailed exploration of Michelson and Mach-Zehnder interferometers within the context of the present paper. Interferometric techniques play a crucial role in optical methods, providing a sophisticated means of studying variations in the refractive index induced by non-uniform temperature fields. These techniques operate on the principle of interference, where coherent light beams are manipulated to create interference patterns, and changes in refractive index can be precisely measured through the analysis of these patterns.

The various theoretical principles for temperature measurements using interferometry have been discussed by Nirala and Anil (1999); they have performed a detailed review of laser-based interferometric techniques for the measurement of the refractive index and temperature. Goldstein and Eckert (1960) measured the heat transfer coefficients of a uniformly heated vertical plate using Mach-Zehnder interferometry. Kang and Herman, 2001 conducted an experimental study using Holographic interferometry combined with high-speed cinematography on the incompressible, moderate Reynolds number flow of air over heated rectangular blocks in a two-dimensional, horizontal channel.

Naylor (2003), in his comprehensive review of recent advancements in interferometric measurements of convective heat transfer rates, explored an approximate beam-averaging approach for extracting heat transfer rates within three-dimensional fields. Additionally, Vani *et al.* 2004 conducted an interferometric study to determine the diffusion coefficient of transparent liquid solutions, utilizing the Michelson interferometer configuration. This research involved the formation of two distinct circular interference fringe patterns resulting from the use of two solutions with different concentrations. The diffusion coefficient was subsequently derived from the time-varying interferograms. Furthermore, Gulshan *et al.* 2023; 2017 and Vijay *et al.* 2019 conducted interferometric measurements in a wide variety of heat transfer applications which showed the potential of these methods in confined spaces.

In the current research project, the primary objective is to thoroughly examine and analyze the temperature distribution within a defined channel, employing both Mach-Zehnder and Michelson interferometric set-ups. The specific channel chosen for this investigation is a rectangular structure with dimensions measuring 4 mm x 4 mm. This carefully selected geometry enables exploring the intricacies of temperature variation in a confined space, mimicking real-world scenarios relevant to various applications such as microfluidics, thermal management and heat exchangers.

Conducting experiments under controlled conditions is a pivotal aspect of our approach. We maintain a constant and predetermined heat input as well as a specific flow rate tailored to the dimensions and characteristics of the chosen channel. This meticulous

control ensures that the observations are consistent and representative, allowing for meaningful comparisons between the Mach-Zehnder and Michelson interferometric configurations. The Mach-Zehnder interferometer, renowned for its capability to manipulate phase differences between arms and provide high-precision measurements, is juxtaposed with the Michelson interferometer, known for its simplicity and sensitivity to changes in optical path length. By implementing both interferometric setups in the same experimental context, it has been aimed to extract comprehensive insights into their respective performances in capturing the nuanced details of temperature distribution along the channel.

The comparative study facilitated by the results obtained from these experiments is of paramount importance. It allows discerning the strengths and weaknesses of the Mach-Zehnder and Michelson interferometer configurations and guides in understanding their applicability and efficiency in different thermal analysis scenarios. This comparative analysis contributes not only to the advancement of interferometric measurement techniques but also aids researchers and engineers in making informed decisions when selecting the most suitable interferometric configuration for specific applications. Furthermore, the outcomes of this research hold potential significance for optimizing thermal management strategies in various technological domains. Understanding how these interferometric setups respond to the thermal dynamics of the channel contributes to the broader knowledge base in heat transfer and fluid dynamics, fostering advancements in fields such as microscale heat exchangers, electronic cooling systems, and biomedical devices. Overall, this investigation lays the groundwork for advancing the understanding of temperature distribution in confined channels, with implications for enhancing the efficiency and performance of diverse technological systems.

2. THEORETICAL DEVELOPMENT

The relation between the density of a homogeneous medium and its refractive index is given by the Lorenz-Lorentz equation,

$$\frac{n^2-1}{\rho\left(n^2+2\right)}=C \qquad \ldots\ldots\ldots\ldots\ldots\ldots\ldots\ldots\ldots\ldots (1)$$

where, C is the Gladstone Dale constant, which is the characteristic of the medium and weakly depends on wavelength. The nanofluid concentration is 0.001%; hence, equations are taken for de-ionized water with significant approximation.

Lorenz-Lorentz relation can be modified by fitting a quadratic polynomial between density and temperature:

$$\frac{n^2-1}{\left(n^2+2\right)}=C\left[-0.0032T^2+1.6415T+795.54\right] \ldots\ldots\ldots (2)$$

The ideal interferometric relation can be written as,

$$n^r - n = \frac{S\lambda}{L} \qquad \ldots\ldots\ldots\ldots\ldots\ldots\ldots\ldots\ldots\ldots (3)$$

where, S is the fringe number, λ is the wavelength of the light source and L is the distance of light travel.

From Eq. (1) and Eq. (3) one will get

$$\left(\frac{-0.0032T_r^2+1.6415T_r+795.94}{-0.0032T^2+1.6415T+795.4}\right)=\frac{1}{(1-aS)} \qquad \ldots\ldots\ldots (4)$$

where,

$$a=\left(\frac{n+1}{n^2+2}\right)\left(\frac{\lambda}{CL}\right)\left(\frac{1}{-0.0032T_r^2+1.6415T_r+795.4}\right) \ldots (5)$$

The reference temperature is the temperature of the fringe adjacent to the unheated upper wall of the channel. After obtaining the reference temperature the temperatures along the direction perpendicular to the wall can be obtained using the stepping procedure as in Eq. (4). From the temperature profile at any location along the channel, the wall heat flux, the heat transfer coefficient and the local Nusselt number are obtained as follows.

$$q_o''(x) = -kw\left(\frac{\partial T}{\partial y}\right)_w \qquad \ldots\ldots\ldots\ldots\ldots\ldots\ldots\ldots\ldots (6)$$

$$h_x = kw\left(\frac{\partial T}{\partial y}\right)_w\left(\frac{1}{T_w-T_m}\right) \qquad \ldots\ldots\ldots\ldots\ldots\ldots\ldots (7)$$

$$Nu_x = \frac{k_w}{k_f}\left(\frac{D_h}{T_w-T_m}\right)\left(\frac{\partial T}{\partial y}\right)_w \qquad \ldots\ldots\ldots\ldots\ldots\ldots\ldots (8)$$

$$T_f = \left(\frac{T_w+T_m}{2}\right) \qquad \ldots\ldots\ldots\ldots\ldots\ldots\ldots\ldots\ldots\ldots (9)$$

Here, T_m is the integral average fluid temperature, calculated using the temperature profile. An integral average heat transfer coefficient is obtained from the local heat transfer coefficients, as shown in Eq. (10). The average Nusselt number is determined from the average heat transfer coefficient, as given in Eq. (11). The thermal conductivity value used in the calculation of the average Nusselt number is evaluated at T_f:

$$h_{av} = \left(1/x\right)\int h \, dx \qquad \ldots\ldots\ldots\ldots\ldots\ldots\ldots (10)$$

$$Nu_{av} = \frac{h_{av} D_h}{k_f} \qquad \ldots\ldots\ldots\ldots\ldots\ldots (11)$$

3. EXPERIMENTAL STUDY

Interferometric techniques are employed in this study to assess the temperature distribution within a channel of 4 mm hydraulic diameter. The utilized interferometric configurations include the Michelson interferometer and the Mach-Zehnder interferometer. A comprehensive examination of these two optical setups and a detailed description of the experimental arrangement are presented in the subsequent sections.

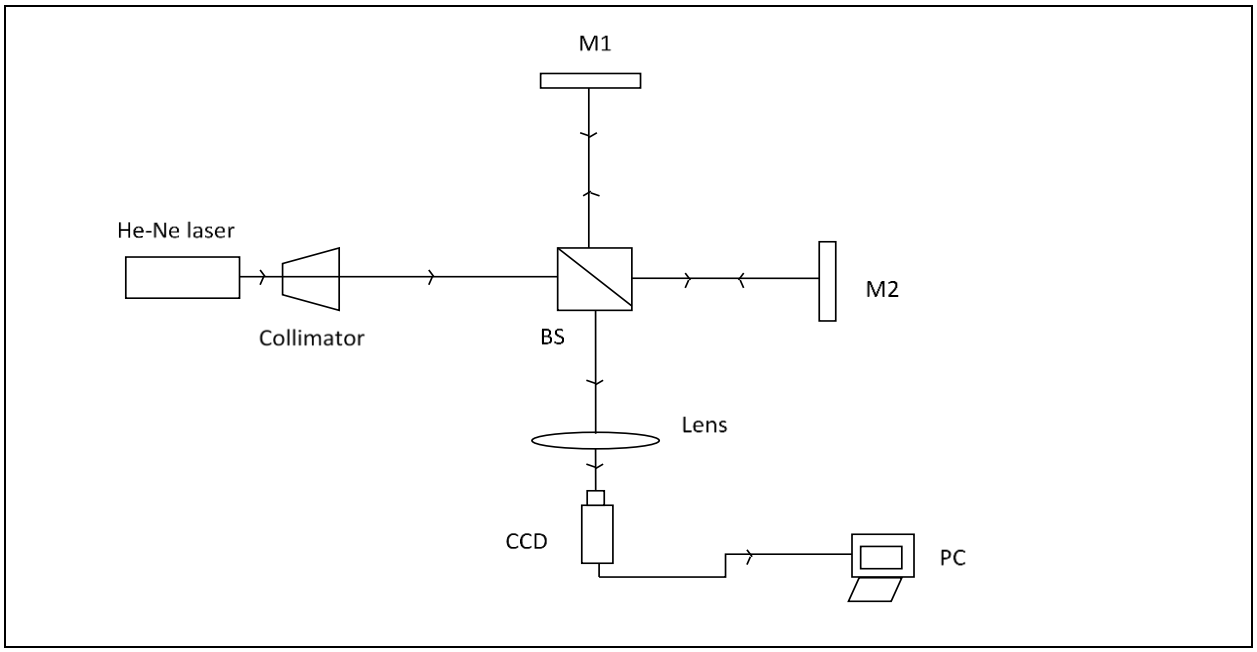

Fig. 1: Michelson interferometer

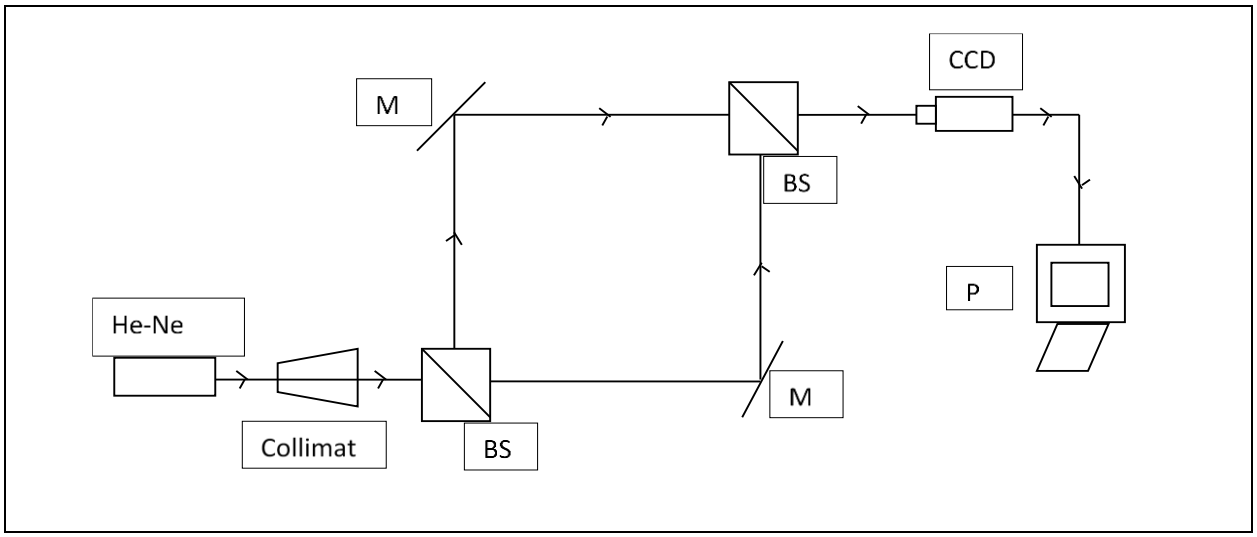

Fig. 2: Mach-Zehnder interferometer

3.1. Michelson Interferometer

The optical configuration of the Michelson interferometer is elucidated in Fig. 1. In this setup, monochromatic light sourced from a He-Ne laser (with a wavelength of 632.8 nm and power of 1.5 mW) is utilized. The He-Ne laser emits light, which, following expansion and collimation, impinges upon the beam splitter (BS), leading to its division into two beams. One of these beams traverses to mirror M1, while the other is directed towards mirror M2. The test section is strategically positioned within one of the interferometer arms, specifically the reflected beam arm. The lights reflected from mirrors M1 and M2 combine, creating the desired interference pattern. These interference patterns are meticulously captured through the application of a CCD camera, integrated with the AVT Fire package software. Subsequently, the acquired images are directly transferred to a PC for comprehensive digital analysis. The digital image analysis is executed utilizing MATLAB 7 software, providing a robust platform for processing and extracting valuable insights from the captured interference patterns in the Michelson interferometric set-up.

3.2. Mach-Zehnder Interferometer (MZI)

The optical configuration of the Mach-Zehnder interferometer is detailed in Fig. 2. Similar to the Michelson interferometer, a He-Ne laser serves as the monochromatic light source, maintaining the specifications with a wavelength of 632.8 nm and a power output of 1.5 mW. The light emitted from the laser undergoes collimation and subsequently impinges on the initial beam splitter (BS1). BS1 effectively divides the light into a reflected beam and a transmitted beam. The reflected beam is directed towards mirror M1, while the transmitted beam is guided to mirror M2. Mirrors M1 and M2 reflect the incident beams, and these reflected beams re-convene at the second beam splitter (BS2). The test section is strategically positioned within one of the interferometer arms, specifically in the reflected arm in this case. The interference fringe pattern, generated as a result of the beams' recombination at BS2, is adeptly captured using a CCD camera. The CCD camera is directly linked to a PC, facilitating the seamless transfer of images for subsequent digital analysis. The acquired images are subjected to meticulous digital analysis using MATLAB 7 software, which serves as a robust tool for processing and extracting pertinent information from the interference patterns observed in the Mach-Zehnder interferometric setup. This comprehensive explanation elucidates the intricate workings of the Mach-Zehnder interferometer and its experimental setup for temperature measurement.

The experimental setup depicted in Fig. 3 is comprehensively composed of several essential components, including the interferometric section, test and reference sections, fluid circulation arrangement and a dedicated temperature measurement unit. Within the scope of this investigation, both Michelson and Mach-Zehnder interferometric configurations, previously outlined, are employed. The test and reference sections consist of identical channels fabricated from high-quality optical glass, featuring a rectangular cross-section measuring 4 mm x 4 mm.

To induce controlled heating within the test channel, a small filament heater is affixed to its bottom side. The input to the heater is precisely regulated using an autotransformer. The working fluid passing through the channels is test fluid. For obtaining reference temperature, a meticulously calibrated T-type thermocouple, equipped with a 20 μm diameter wire, is inserted into the channel and aligned on the reference fringe. The thermocouple data is systematically acquired utilizing an Agilent 34970 data acquisition system, seamlessly interfaced with a PC for efficient data processing.

The circulation of fluid through both the test and reference channels is facilitated by a solenoid-operated plunger pump. The flow rate is quantified through the integration of a rotameter into the hydraulic circuit. To maintain laminar flow conditions, the mass flow rate is precisely controlled using a needle valve. The intricate interference fringe patterns generated are captured using a CCD camera, integrated with the AVT Fire package software. These images are then subjected to digital analysis through MATLAB 7 software, ensuring a comprehensive and sophisticated approach for extracting valuable insights from the interferometric data obtained during the experiment.

4. RESULT AND DISCUSSION

In this study, a series of experiments were undertaken employing two distinct interferometric set-ups, as delineated in the preceding sections. The experimental investigations were centered around a sample test section characterized by a hydraulic diameter of 4 mm, consistent across both set-ups. Specifically, the sample test section comprised a channel designed to facilitate laminar flow, and the experimental conditions were standardized with a flow rate of 15 lph (liters per hour) and a heat input of 60 W. In the laminar flow regime, the chosen flow rate of 15 lph ensured a

controlled and stable fluid flow within the channel. The heat input of 60 W was precisely applied to the bottom surface of the channel, inducing a localized heating effect. Consequently, the initial interference fringes within the channel, originally parallel to the bottom surface, underwent discernible deflection. This deflection was directly proportional to the heat dissipation occurring from the channel surface, providing valuable insight into the thermal behavior of the system

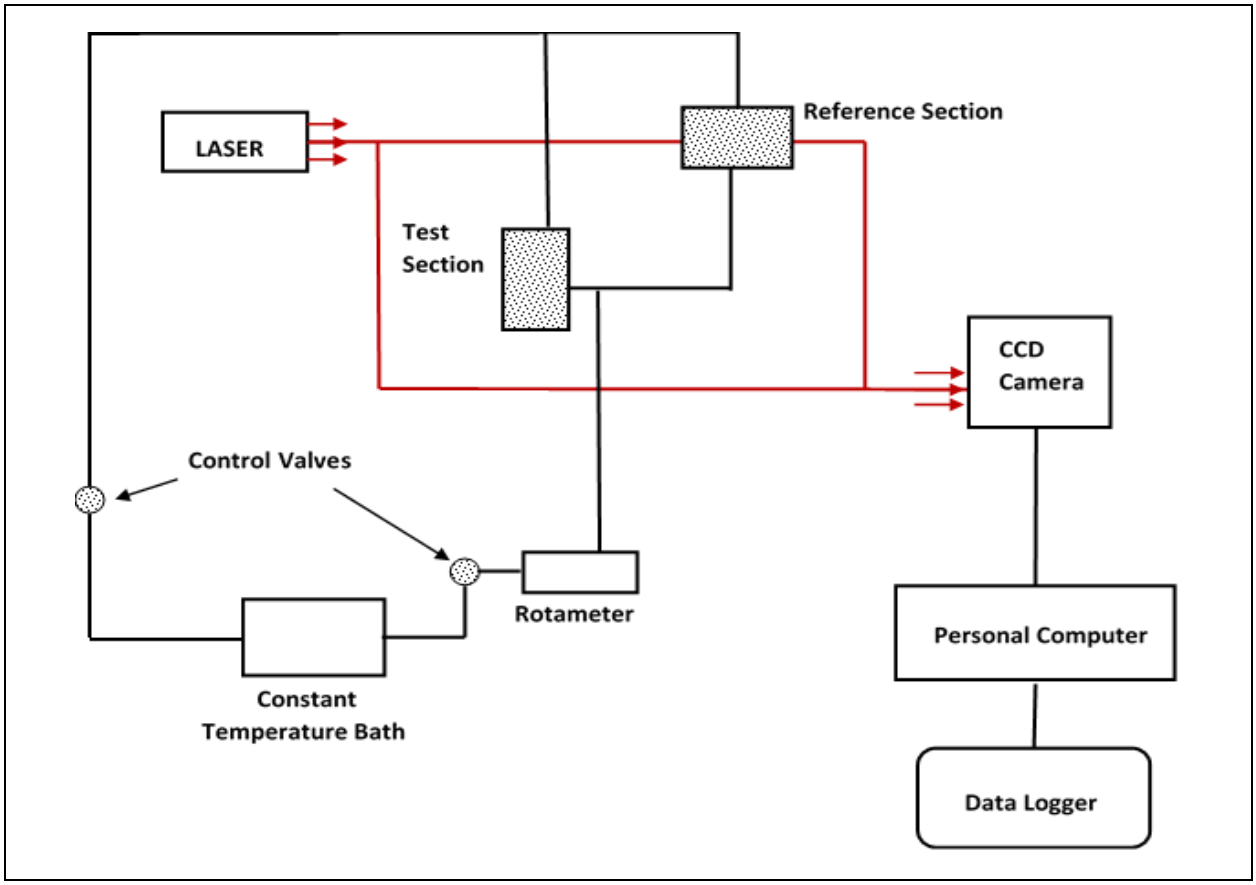

Fig. 3: Schematic diagram of experimental arrangement

To capture and analyze the intricate details of the temperature distribution along various sections of the channel, a digital image processing technique was employed on the interference fringes. The interference fringes served as a visual representation of the temperature variations induced by the applied heat. By leveraging digital image processing, the researchers were able to extract quantitative information regarding the temperature distribution across different regions of the channel. The results of these experiments were then visualized through the fringe patterns obtained from both the interferometric setups. The Michelson and Mach-Zehnder interference patterns obtained for the specific conditions of 60 W heat input and 15 lph flow rate were subsequently examined and compared. These visualizations provided valuable insights into the thermal characteristics of the system under investigation and contributed to a comprehensive understanding of heat dissipation and fluid behavior in the mini channels studied.

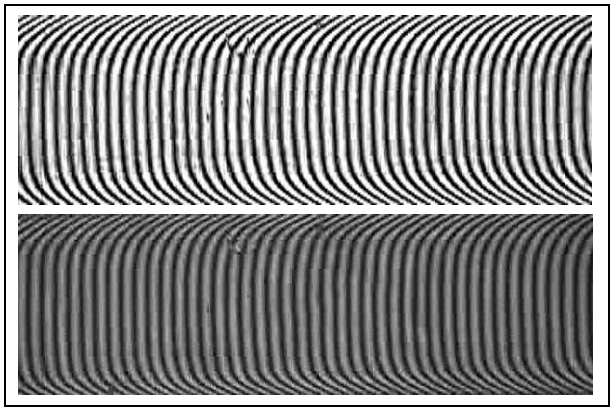

Fig. 4: Typical fringe patterns obtained using Michelson and Mach-Zehnder interferometers for 3 mm hydraulic diameter channel

The utilization of MATLAB in the experimental analysis involved a detailed exploration of the pixel-level information within the acquired images. MATLAB, being a powerful numerical computing environment,

allowed for the extraction and manipulation of pixel values at each point throughout the images. This capability enabled a granular understanding of the spatial characteristics present in the images, which were crucial for unraveling the underlying physical phenomena. To establish a meaningful correspondence between pixel values and actual physical distances, a calibration process was executed. This process took into consideration the known width of the channel. By employing this calibration, the pixel values were systematically converted into real-world physical distances. This conversion was fundamental for accurately mapping the intensity variations across the images onto the physical dimensions of the experimental set-up. Following the calibration, an intensity profile was systematically generated for different vertical sections along the channel length. This profile represented the variations in pixel intensity, providing a visual depiction of the brightness or intensity distribution within the channel. The intensity profile served as a valuable tool for understanding how heat or other physical parameters were distributed spatially along the cross-section of the channel.

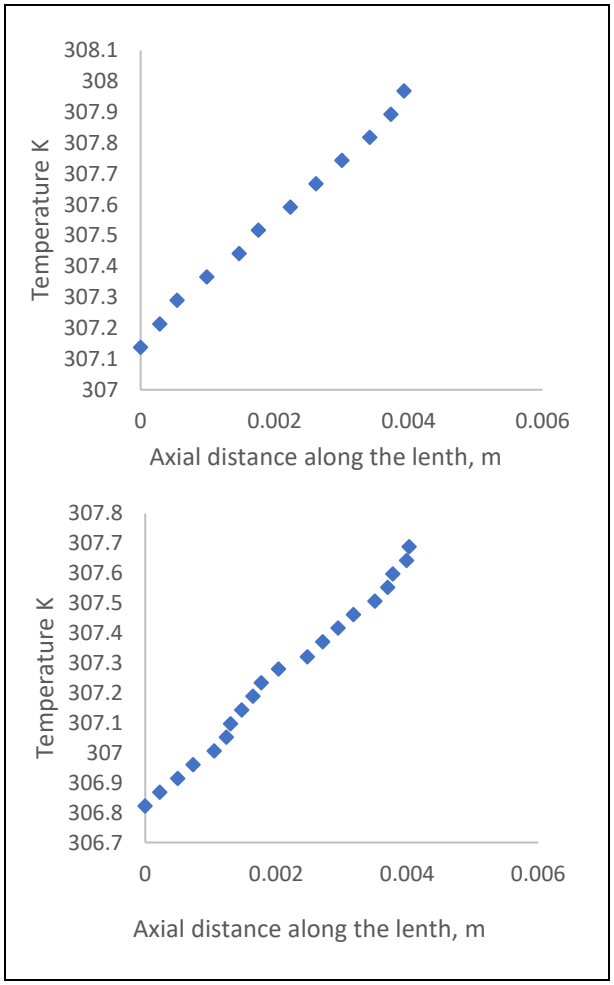

Fig. 5: Temperature distribution along a vertical section in the test section by Mach-Zehnder and Michelson methods, respectively

Fig. 5 illustrates the temperature distribution within both Michelson and Mach-Zehnder Interferometer (MZI) configurations, specifically corresponding to the 320th pixel along the channel length. This pixel serves as a representative point for the thermal analysis, and a similar methodology can be applied to derive the temperature distribution along the vertical direction across the entire length of the channel. The principles outlined in Section 2 guide the extraction of crucial heat transfer parameters from these interferometric measurements.

The discussion in this study revolves around two conventional interferometric configurations, namely Michelson and MZI, highlighting their application to a specific thermal problem. The temperature trends depicted using these interferometric techniques exhibit a commendable agreement with theoretical predictions available in the existing literature. This alignment underscores the reliability and accuracy of the chosen interferometric setups for temperature measurement in the experimental context. The MZI configuration, a well-established technique for temperature measurements, is characterized by its precision and reliability. In contrast, the Michelson interferometric configuration is noted for its simplicity, employing fewer optical components and facilitating an easier setup. This streamlined setup not only simplifies the experimental arrangement but also minimizes potential errors arising from imperfections in optical components. The configuration's unique feature, involving the scanning of the test section twice by the light beam, contributes to enhanced accuracy in temperature measurements.

5. CONCLUSION

The application of a wedge fringe setting in both interferometer set-ups adds to the versatility and practicality of the experimental arrangement. Notably, the wedge fringe setting does not necessitate high-quality optics or extremely precise alignment, making it a practical choice in experimental setups. This feature is particularly advantageous in minimizing potential sources of error, contributing to the robustness of the interferometric measurements. To enhance the accuracy and reliability of the temperature measurements, digital image processing techniques facilitated by MATLAB were employed. This sophisticated analytical tool ensures precise extraction and interpretation of pixel values, converting them into meaningful temperature distributions. The integration of digital image processing techniques elevates the measurement process, providing a level of accuracy and reliability crucial for understanding intricate thermal dynamics within the experimental set-up. In summary, the detailed exploration of temperature distribution using Michelson and Mach-Zehnder configurations, supported by robust theoretical agreement, underscores the suitability of these interferometric techniques for the specific thermal

problem at hand. The advantages of each configuration, coupled with the practicality of the experimental setup and the precision offered by digital image processing, collectively contribute to the accuracy and reliability of the temperature measurements obtained in this study.

ACKNOWLEDGMENTS

The optimization reported in the present work were built with the financial support received from the Science and Engineering Research Board (SERB) (Power Grant), India through the Grant ID SPG/2021/000822. The authors acknowledge the support received from SERB, India.

FUNDING

This research received financial support from the Science and Engineering Research Board (SERB) (Power Grant), India through the Grant ID SPG/2021/000822.

CONFLICTS OF INTEREST

The authors declare that there is no conflict of interest.

COPYRIGHT

REFERENCES

Ayoub, A., Norris, S. E. and Rajnish, N. S., Heat transfer measurement techniques in microchannels for single and two-phase Taylor flow, *App. Thermal Engg.*, 162, 114280 (2019). https://doi.org/10.1016/j.applthermaleng.2019.114280

Cardone., G. M. and Gennaro, C., Infrared thermography for convective heat transfer measurements, *Exp. Fluids.*, 49, 1187–1218 (2010). https://doi.org/10.1007/s00348-010-0912-2

Dennis, R. J., Gary, S. S. and Michael D. T., Schlieren "PIV" for turbulent flows, *Optics Lasers Engg.*, 44(3-4), 190-207 (2005). https://doi.org/10.1016/j.optlaseng.2005.04.004

Eckert, R. J. and Goldstein, E., The steady and transient free convection boundary layer on a uniformly heated vertical plate, Int. *J. Heat Mass Tran.*, 1(2-3), 208-210 (1960). https://doi.org/10.1016/0017-9310(60)90023-5

Gannavarpu, Sreeprasad, A. and Rajshekhar, Non-invasive precision metrology using diffraction phase microscopy and space-frequency method, *Optics Lasers Engg.*, 109, 17-22 (2018). https://doi.org/10.1016/j.optlaseng.2018.05.005

Gulshan, K. S., Sunhash, K U., Arjun, P., Surya, N., Arun, A. and Atul, S., Imaging Convective Phenomena inside Highly Refractive Cylindrical Enclosures, *Heat Tran. Engg.*, 45(1), 40-54 (2023). https://doi.org/10.1080/01457632.2023.2171812

Mohammed, H.A., Gunnasegaran, P. and Shuaib, N.H., Influence of channel shape on the thermal and hydraulic performance of microchannel heat sink, Int. Comm. *Heat Mass Transfer.*, 38(4), 474-480 (2010). https://doi.org/10.1016/j.icheatmasstransfer.2010.12.031

Mohammed, H.A., Gunnasegaran, P. and Shuaib, N.H., Numerical simulation of heat transfer enhancement in wavy microchannel heat sink, *Int. Comm. Heat Mass Transfer.*, 38(1), 63-68 (2011). https://doi.org/10.1016/j.icheatmasstransfer.2010.09.012

Lee, J. and Mudawar, I., Low-temperature two-phase microchannel cooling for high heat-flux thermal management of defense electronics, *IEEE Tran Comp Pack Tech.*, 32(2), 453–465 (2009). https://doi.org/10.1109/TCAPT.2008.2005783

Jagadesh, R., Tullio, D. R., Rajshekhar, G. and Dario, A., Quantitative flow visualization by hidden grid background oriented schlieren, *Optics Lasers Engg.*, 160, 107307 (2023). https://doi.org/10.1016/j.optlaseng.2022.107307

Kang and Herman, C. E., Experimental visualization of temperature fields and study of heat transfer enhancement in oscillatory flow in a grooved channel, Heat *Mass Transfer.*, 37, 87–99 (2001). https://doi.org/10.1007/s002310000101

Pedram, M. and Nazarian, S., Thermal Modeling, Analysis, and Management in VLSI Circuits: Principles and Methods, *Proc. IEEE.*, 94(8), 1487–1501 (2006). https://doi.org/10.1109/JPROC.2006.879797

Merzkirch, A. H. and Wolfgang, Investigation of the properties of a sharp-focusing schlieren system by means of Fourier analysis, *Optics Lasers in Engg.* 44, 159-169 (2006). https://doi.org/10.1016/j.optlaseng.2005.04.003

Mirko, Z., Joshua B. E. and Gennaro C., A general procedure for infrared thermography heat transfer measurements in hypersonic wind tunnels *Int. J. of Heat Mass Transfer.*, 163, 120419 (2020). https://doi.org/10.1016/j.ijheatmasstransfer.2020.120419

Naylor, D., Recent developments in the measurement of convective heat transfer rates by laser interferometry, *Int. J. Heat Fluid Flow.*, 24(3), 345-355 (2003). https://doi.org/10.1016/S0142-727X(03)00021-3

Nirala, Chandra, S. and Anil K., 1999. A review on refractive index and temperature profile measurements using laser-based interferometric techniques, *J. Optics Lasers Engg.*, 31(6), 455 – 491(1999). https://doi.org/10.1016/S0143-8166(99)00037-8

Pease, D. B. and Tuckerman, R. F. W., High-performance heat sinking for VLSI, *IEEE Electron Device Lett.*, 2 (5), 126 – 129 1(1981). https://doi.org/10.1109/EDL.1981.25367

Gulshan, K, S., Rahul, H. D., Divya, H. and Atul, S., Performance evaluation of compact channels with surface modifications for heat transfer enhancement: An interferometric study in developing flow regime, *Int. J. Heat Fluid Flow*., 64, 55-65 (2017). https://doi.org/10.1016/j.ijheatfluidflow.2017.02.002

Vani, K. C., Arun, A., and Narayanamurthy, C. S., Imaging Convective Phenomena inside Highly Refractive Cylindrical Enclosures, *Optics Lasers Engg.*, 42 (1), 9-20 (2004). https://doi.org/10.1016/j.optlaseng.2003.07.005

Vijay, S., Divya, H., and Atul S., Experimental study of heat transfer performance of compact wavy channel with nanofluids as the coolant medium: Real time non-intrusive measurements, *Int. J. Thermal Sci.*, 145, 105993 (2019). https://doi.org/10.1016/j.ijthermalsci.2019.105993

Wei, X. and Joshi, Y., Stacked microChannel heat sinks for liquid cooling of microelectronic components, *J. of Electronic Packaging, Tran. of the ASME.*, 126(1), 60-66 (2004). https://doi.org/10.1115/1.1647124